

Chapter 3

Seebeck Metrology

The Seebeck coefficient is unique to the metrology of thermoelectric materials. While the purely thermal transport properties (c_p , D_T , and κ) and the electrical properties measured using the Van der Pauw method (n_H , σ , and μ_H) are essential to thermoelectric characterization, they are also essential to other fields of scientific inquiry. For this reason Seebeck metrology is far less advanced and far less understood than that of the other variables, though great effort is being made by many to rectify that shortcoming. [47, 130, 94, 90]

On my first day working at the Caltech Thermoelectrics Group I was introduced to a moth-balled pair of Seebeck metrology devices and asked to restore them to full functionality. I spent many hours calibrating these systems and I eventually constructed my own Seebeck measurement system with the help of my undergraduate assistant David Neff. Over this time I learned many of the details and potential failings of Seebeck metrology.

This understanding of Seebeck metrology was essential to the work presented in this thesis. The materials that I studied were substantially more difficult to measure than typical thermoelectric materials. The Seebeck coefficient has a much stronger first and second temperature derivative near its phase transition temperature, requiring greater stability and resolution. To illustrate this I plot in Figure 3.1 both the Seebeck coefficients of Cu_2Se and $\text{Na}_{0.01}\text{Pb}_{0.99}\text{Te}$ [153] on the same axis.

The presence of the phase transition itself warrants more detailed investigation. The structural transformations of a phase transformation may be associated with

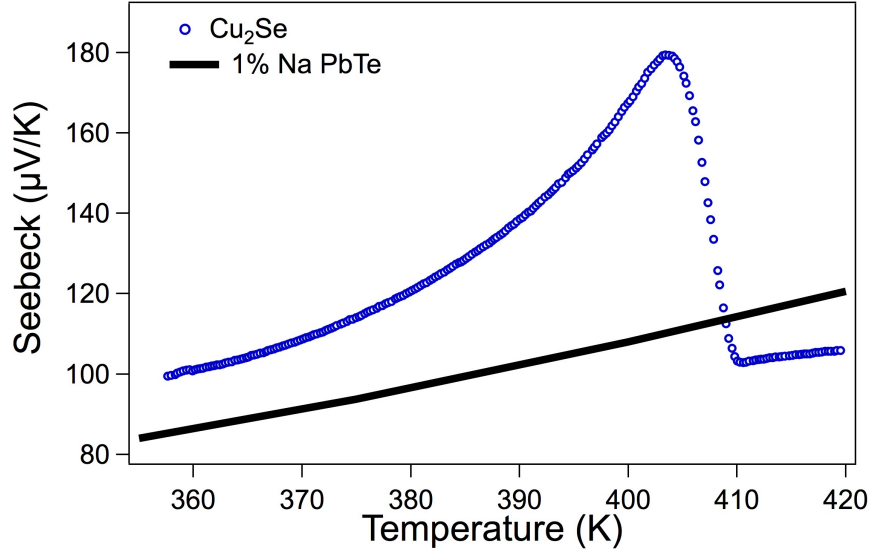


Figure 3.1: Seebeck coefficient of Cu_2Se compared with that of $\text{Na}_{0.01}\text{Pb}_{0.99}\text{Te}$. Cu_2Se 's strong peak near its phase transition requires more precise measurement than is typical for thermoelectric materials. PbTe data courtesy of Yanzhong Pei [153].

time dependent kinetics. These time dependent kinetics may result in chimerical transport properties.

3.1 Measuring the Seebeck Coefficient

The essence of a Seebeck measurement is to measure the voltage difference (ΔV) across a sample under a fixed temperature gradient (ΔT) at some fixed temperature \bar{T} . The Seebeck coefficient (α) is then taken as $\Delta V/\Delta T$; this quantity I shall sometimes refer to as the *nominal Seebeck coefficient* or α_m . By convention ΔV is defined at the voltage on the cold side minus the voltage on the hot side, while $\Delta T = T_h - T_c$. Both the voltage and temperature are measured at the same nominal point on the sample. This is done by pressing one thermocouple onto a hotter point of the sample and one thermocouple onto a colder point on the sample, see Figure 3.2. The Seebeck coefficient is, as defined in Equation 1.1 is actually the ratio of the *gradients* of V and T . Single point Seebeck measurements are therefore an approximation to $\Delta V/\Delta T \approx \nabla V/\nabla T$. This may cause an error and these errors are discussed in the context of typical metrology techniques below in reference to Cu_2Se . It will be shown

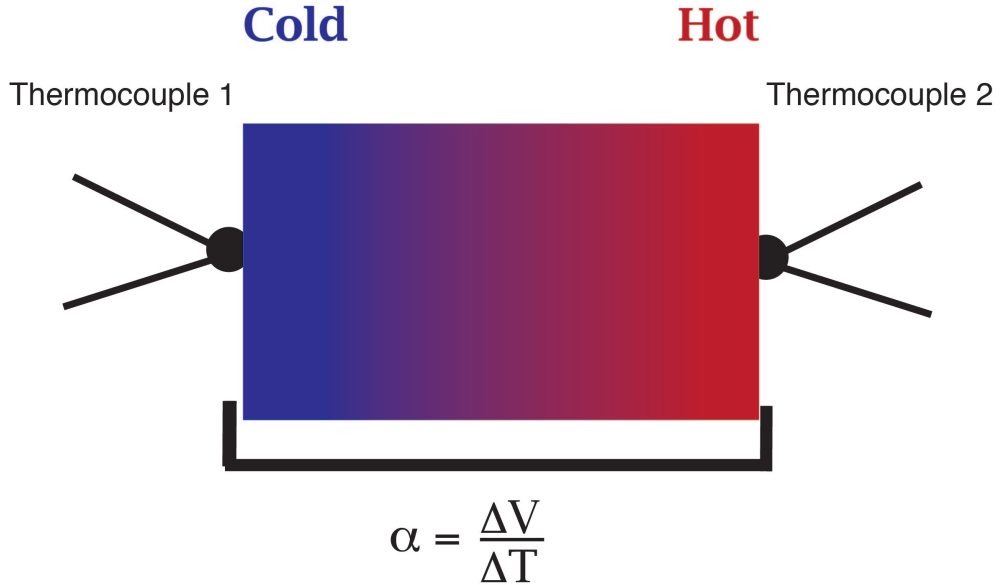


Figure 3.2: Schematic of a Seebeck measurement. Two thermocouples are placed at two different points on a sample. Both ΔT and ΔV are measured with the thermocouples. In a single point measurement $\Delta V/\Delta T$ is taken as the Seebeck coefficient.

that these errors are of greater concern near the super-ionic phase transitions studied for this thesis.

A more pernicious and frequently large error is the small voltage measured even when $\Delta T = 0$ [90, 129]. This offset is colloquially referred to as the dark voltage, V_D , though one should not be misled into thinking it is a voltage error. It may be caused by error in temperature measurement. That quantity I refer to as the dark temperature. It is defined as the ΔT for which $\Delta V = 0$ and is related to V_D by $T_D = V_D/\alpha$. The intercept error, whether formulated as T_D or V_D , is problematic for single point Seebeck measurements. The error induced is determined by:

$$\alpha_m = \alpha \left(1 + \frac{T_D}{\Delta T} \right) \quad (3.1)$$

Because of this error single point Seebeck metrology is no longer used. An example is discussed in section 3.3 in the context of Cu_2Se [144].

To compensate for these variations on the *oscillation* Seebeck measurement is

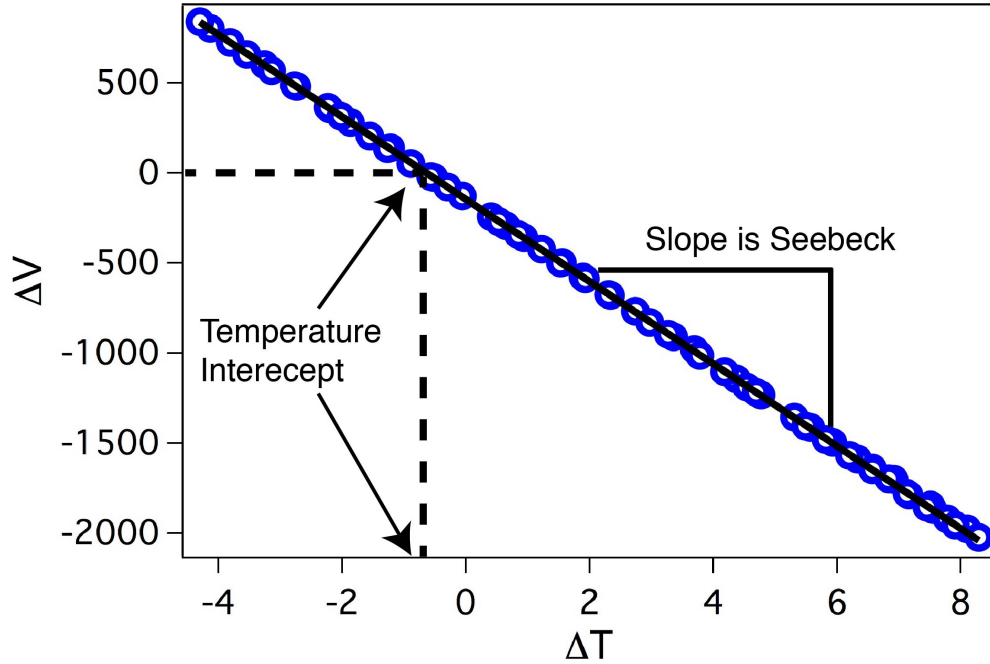


Figure 3.3: Raw Seebeck data from an oscillation sequence. The slope of the data is taken as the Seebeck coefficient.

now used almost universally [47, 94]. In this technique ΔT is varied while \bar{T} is held constant and ΔV is measured. The resulting data is plotted as in Figure 3.3 and a line fit to it. This compensates for T_D , which is the intercept of such a plot. The slope of that line is taken α , though errors other than T_D may still effect its value. These issues are discussed more explicitly later in this chapter.

Measuring Seebeck coefficient correctly is technically challenging partially due to a lack of standardized samples. Though many metals used in thermocouples are well calibrated, they have relatively low Seebeck coefficient (*e.g.*, $10 \mu\text{V}/\text{K}$) and high thermal conductivity (*e.g.*, $50 \text{ W}/\text{m} \cdot \text{K}$). Good thermoelectrics have a much higher Seebeck (*e.g.* $\alpha > 100 \mu\text{V}/\text{K}$) and lower thermal conductivity ($\kappa < 3 / \text{m} \cdot \text{K}$). Due to the great mismatch between the thermal conductivities of metals and good thermoelectrics, an apparatus designed for one will be inappropriate for the other. Round robin testing has lead to the development of a Bi_2Te_3 standard below 400 K [124, 126, 125]. No such standard is available at higher temperatures, though such standards are under current development at both NIST [125, 131] and ORNL [195].

The Seebeck of Bi_2Te_3 standard varied by 5% from lab to lab during the round-robin test [124], and I take this as the current upper limit of accuracy for Seebeck metrology.

The lack of standards for Seebeck measurement means care must be taken in instrumentation design. A Seebeck measurement may have low Gaussian noise but still exhibit large systematic errors. For example, Dr. Joshua Martin at NIST has made a strong case that instruments designed using an infrared furnace, such as that of the commercially available ULVAC ZEM-3 and Linseis LSR-3, produce repeatable errors in Seebeck measurement [94]. Dr. Johannes de Boor of DLR in Germany found that systematic error may be present in data for which the linear fit has $1 - R^2 < .01$; further order of magnitude reductions in the deviation of R^2 from unity resulted in systematically improved data [47]. Correct apparatus design is therefore crucial for accurate Seebeck metrology.

The principle challenge of Seebeck measurement is accurate thermal measurement rather than accurate voltage measurements. Determination of the electrical contact to be ohmic and small is insufficient for determination of good thermal contact [94]. In making a Seebeck measurement it is assumed that the temperature of the thermocouple is the temperature at a particular point on the sample. If there is a combination of heat flux to or through the thermocouple and a thermal resistance from the sample point to the measurement point on the thermocouple, then an error will result. Because the heat flux through the thermocouple tip is driven by the system's various parasitic couplings to low or ambient temperature, this is referred to as the *cold finger effect*. A good Seebeck metrology apparatus reduces the cold finger effect.

There are three standard designs (Figure 3.4) of a thermocouple measurement apparatus commonly used today. The first is the *two point* design, in which the sample is sandwiched between electrically conductive heater blocks and the electrical and thermal properties measured from within the blocks. The second is the *four point linear* design in which the thermocouples touch the sample from its side instead of being inside the heater block. The final design, which was created by NASA JPL in support of their radio-isotope thermal generator program [90], is the *four point co-linear* design. Like in the four point design, the thermocouples directly touch the

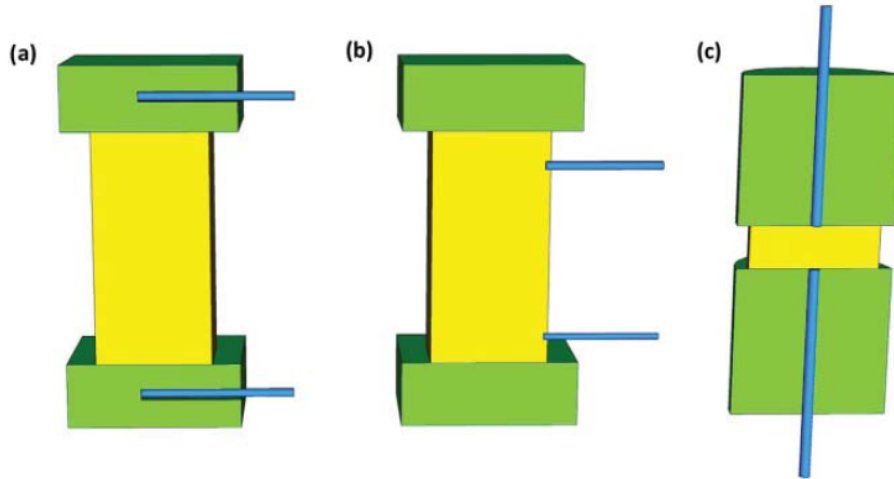


Figure 3.4: The three principle Seebeck geometries. Sample is shown in yellow, heater block in green, and thermocouple in blue. (a) the two point linear design. (b) the four point linear design. (c) the four point co-linear design. Image adapted from Iwanaga *et al.* [90].

sample, but here they pass through the heater block. The four point co-linear design was used for this experiment.

The two point design (Figure 3.4(a)) is the most traditional as it is relatively easy to construct. In this design the thermocouple can be extremely well thermalized to the block and that should mitigate its coupling to cold or ambient temperatures. However, while the thermalization with the heater block is excellent, the thermalization to the sample itself is problematic. As a result, two point designs consistently over-estimate ΔT and therefore under-estimate the Seebeck coefficient. The apparatus used in this experiment had thermocouples both in the heater block approximately 1 cm from the sample and thermocouples in direct contact with the sample. As shown in Figure 3.5, the thermocouples in the heater block had a small offset from those touching the sample. Although it only causes a small error in absolute temperature, there is a much more significant (30% here) difference between the ΔT in the blocks and at the sample.

The four point linear design (Figure 3.4(b)) is used in commercial systems such as the ULVAC ZEM-3 and Linseis LSR-3. It is popular because it can be used for

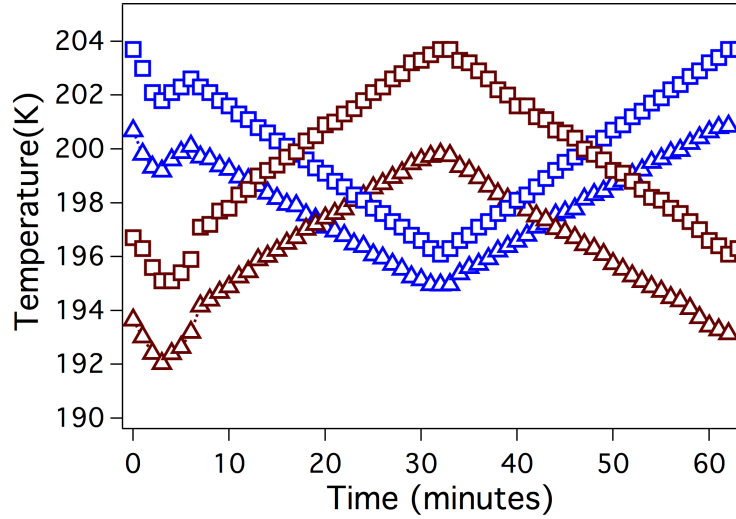


Figure 3.5: Temperature readings on the sample and in the block as ΔT is varied. Magenta represents thermocouples on the top side. Blue represents thermocouples on the bottoms side. Squares represent thermocouples in the heater block while triangles represent thermocouples in direct contact with the sample.

near simultaneous measurement of electrical conductivity and Seebeck coefficient. Its principle flaw is the cold finger effect. The thermocouples do not run through the heater block and so are thermalized via their signal path to the ambient environment. While in theory this may be mediated by heat sinking the thermocouple wires to a hot block, in practice these instruments are only thermalized using an infrared furnace. As a result they tend to underestimate ΔT and therefore overestimate Seebeck. Work at NIST constructing a system with the same configuration found that an overestimate of up to 15% in Seebeck coefficient may result at high temperatures [94] This casts into doubt some of the highest zT s reported as very many of them were measured on ZEM-3s.

The four point co-linear design (Figure 3.4(c)) is meant to include the best features of the other two designs without their defects. The thermocouples contact the sample without intermediation by the heater block as in the four point linear design. The thermocouples are well heat sunk into the heater block itself, as in the two point design. Together these should mitigate both the thermal resistance from sample to thermocouple and minimize the heat flux from the thermocouple into the bath.

However, there may still be temperature fluxes through the thermocouple if there are non-uniformities in the temperature of the block. Such differences have been observed in our apparatus, see Figure 3.5. The temperature difference in the block in that measurement was 30% higher than that at the sample surface.

A simple method for improving thermal contact is the use of a thin graphite-base foil (brand name *grafoil*) between the sample and the pair of block and thermocouples. Due to the conformation of the flexible foil to both sample and thermocouple, the effective thermal contact area is increased and thermal contact resistance decreased. Furthermore, the improved thermal contacts between the heater block and the sample ensure that the best path for thermal conduction goes directly into the block instead of into the thermocouple. The grafoil may cause a small underestimate in ΔT . As the grafoil is only 100μ thick with a thermal conductivity of 10 W/mK , its thermal resistance is a small fraction of sample thermal resistance (less than 2%). The effect on the measured ΔT is therefore negligible.

The consistency of thermal contacts may be tested by measuring the Seebeck both at ambient pressure and under vacuum. Ambient pressure mediates the contact between sample, heater blocks, and thermocouples, thereby reducing the sample thermal contact resistance. Dr. Martin at NIST tested this effect both with and without the use of grafoil to mediate the contact, see Figure 3.6. When no grafoil was present, reducing the pressure from atmosphere to rough vacuum resulted in a 10% shift in the measured value of Seebeck. This 10% shift was eliminated by the inclusion of grafoil contact. The foil also acts as a diffusion barrier to protect the sample and the thermocouple from chemical reactions. Given the high diffusivity of Ag and Cu into other materials, this is an important concern for this work in particular.

3.2 Apparatus and Protocols

The Seebeck apparatus used in this experiment is diagrammed in Figures 3.7(a), 3.7(a). This diagram was originally published in Iwanaga *et al.* [90]. A photograph of the actual apparatus is displayed in Figure 3.7(b). In describing it I will refer to the

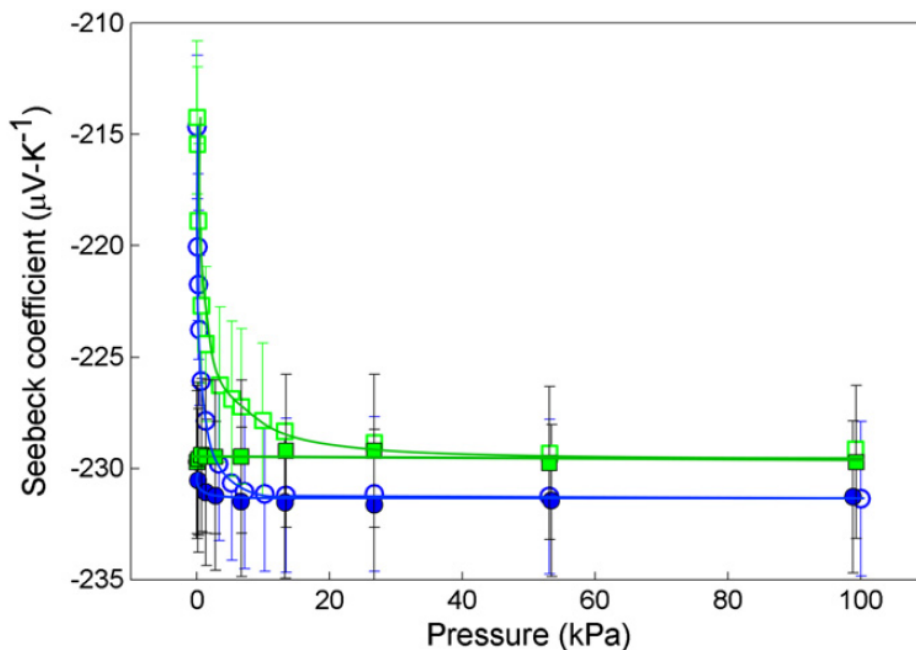


Figure 3.6: The effect of ambient pressure on measured Seebeck. Seebeck coefficient as a function of helium (circles) and nitrogen (squares) gas pressure at 295 K for Bi_2Te_3 SRM 3451 measured under a poor thermal contact (unfilled circles) and the Seebeck coefficient using a graphite-based foil interface (filled circles). Image from Martin *et al.* [131].

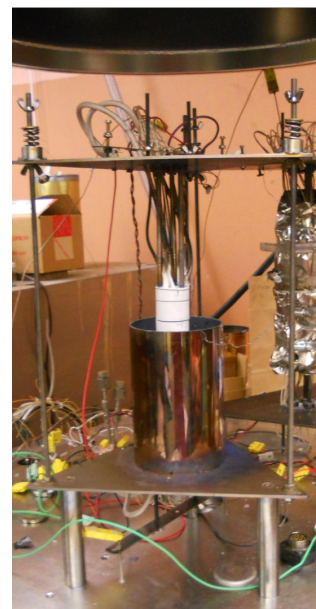
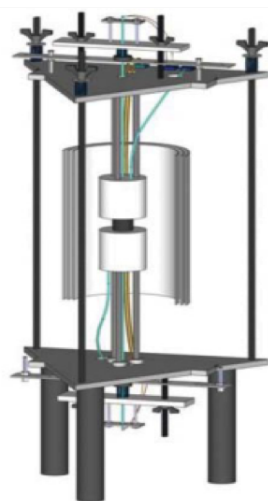
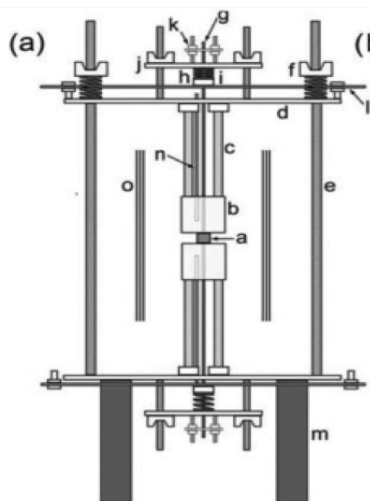


Figure 3.7: Diagram of Seebeck apparatus in profile (a) and three-quarter view (b). Photograph of apparatus used in this research (c). Figures part (a) and (b) were previously published in Iwanaga *et al.*[90]

labels within Figure 3.7(a). The sample (a) is compressed between two cylindrical Boron Nitride (Saint Gobain AX05) heater blocks (b) by three springs (f) pushing through a top plate (d) and three Inconel rod (c). The Boron Nitride blocks contain six symmetrically placed heater cartridges. The measurement thermocouples (g) run through the centers of the heater blocks in order to thermalize them and eliminate the cold finger effect. Compression of the thermocouple onto the sample for good contact is achieved by a spring (h) and plate (i) combination. The thermocouple apparatus is mechanically connected to the top plate by two threaded rods (j). The relative position of the thermocouple is adjusted by two wingnuts pushing on a small plate. The small plate is connected mechanically to the thermocouple by a spring (h). Adjustment by the wingnuts and spring are minor compared with constructing the thermocouple such that the length between the spring and the thermocouple tip is appropriate. An error of one quarter of an inch in this aspect of thermocouple construction will result in an insurmountable error. The thermocouple is put on and removed from the sample via holdoff bolts (l).

The loading procedure for the system is as follows. Wingnuts are located underneath the top plate and are used to separate the two boron nitride blocks without external mechanical support (*e.g.*, the user's arm). If the thermocouples are extended by releasing the hold-offs (l), they should extend 2-4 mm out of the block. The wingnuts for the thermocouples (j) should be set such that the thermocouple can be pushed back mechanically with a single finger with 3-5 pounds of force. If the thermocouple extends less than 2 mm out of the block than the thermal contact may be too poor, and it may even lose contact at higher temperatures due to the thermal expansion of the block. If the thermocouple extends too far it will require too great a force to contract it — Hooke's law being proportional to displacement. This will result in mechanical degradation of the thermocouple tip. The thermocouple tip should be cleaned with isopropanol using a tweezer and a folded Kimwipe in the same gentle fashion by which optical lenses are cleaned. Then the thermocouple holdoffs should be re-engaged.

The sample should then be sandwiched between two pieces of graphoil cut to

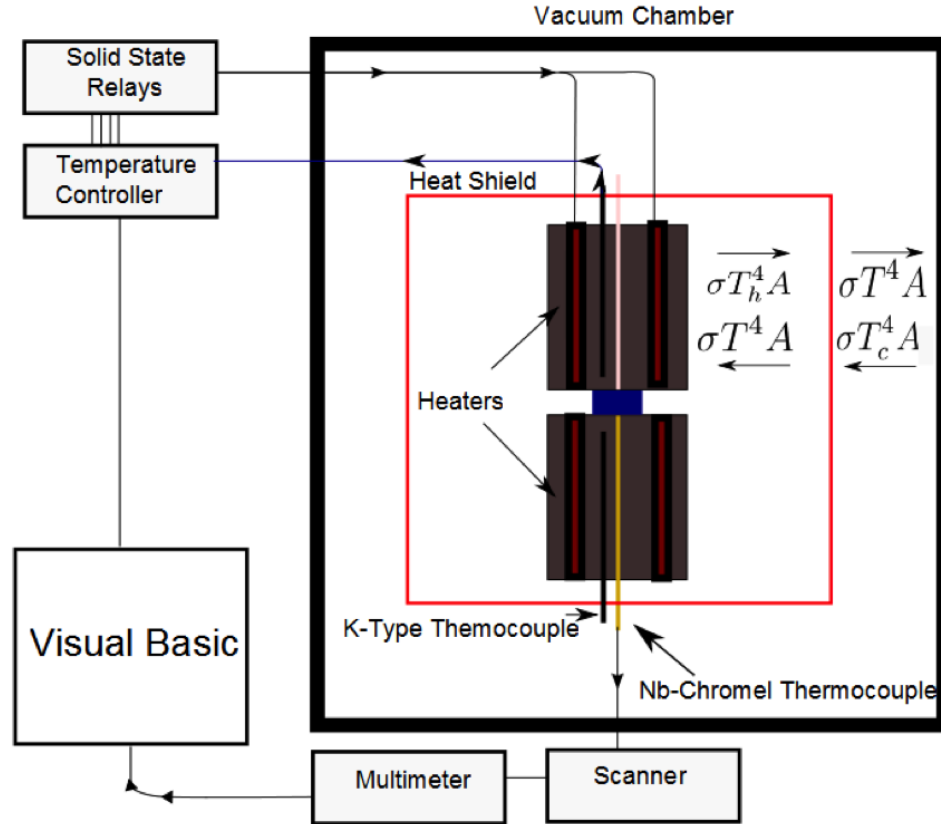


Figure 3.8: Schematic of the measurement and control software used.

the appropriate size and placed on the center of the bottom heater. The top heater should then be carefully lowered onto the top side of the sample. One hand should gently stabilize the top heater block while the other hand lowers the top plate (d) and adjusts the top wingnuts (f). Once the top heater block is on top of the sample the top plate wingnuts (f) should be tightened until resistance is felt. Then each should be tightened by one half a turn; this tightening should be done three times. This will ensure firm contact between the sample and the heater block. Then the thermocouple hold-offs should be disengaged. The heat shield (n) should then be tied onto the threaded rods (e) above the top plate. On occasion — for example, immediately after new thermocouples are installed — the Seebeck should be tested just above room temperature (40 to 50 °C) both in air and in vacuum to ensure that the pressure is sufficient to overcome the thermal contact errors described above.

A schematic of the measurement and control instrumentation for the apparatus

is shown in Figure 3.8(a). The measurement and control electronics and sensors are kept completely separate. Custom thermocouples with a combination of Niobium and Chromel are used to measure the sample. The thermocouple wires exit to a thermocouple scanner card that includes an aluminum block with built-in resistive thermal device (RTD). To measure the temperature on each side of the sample, the voltage from that channel is read on a multimeter. That voltage and the temperature of the cold junction block are input into a look-up table by which the temperature at the thermocouple tip is obtained. The voltage is obtained via the Niobium wires. Niobium was chosen for its relatively low Seebeck coefficient as the Seebeck voltage must be compensated for during measurement.

A k-type thermocouple inserted separately in the block is used to measure and control its temperature. The k-type thermocouples output is connected directly to an Omega CN7000 temperature controller. This value and the temperature set-point allow for PID control of the heater cartridges in the heater block. The heaters are resistive elements that are powered directly from the wall through solid state relays. The PID controllers alter the duty cycle time of the solid state relays and therefore the thermal power. All control is computer controlled through a Visual Basic program written by Dr. G. Jeffrey Snyder with some modifications by this author to deal with particular challenges. At present the author has begun the process of transitioning to python-based control software.

Above 300 °C the dissipation of heat in the system is driven by black body radiation. This was empirically determined via linear fitting of input power and the fourth power of temperature (Figure 3.9) with fitting coefficient $R = 0.99459$. The scatter in the data is due to the functioning of the PID control system. Blackbody radiation may cause thermal fluxes out of the side of the heater block and induce a temperature offset between the two thermocouples and lead to cold finger errors. For this reason heat shielding is installed in the apparatus. In later revisions radiation heat shielding was replaced with direct thermal insulation of the apparatus.

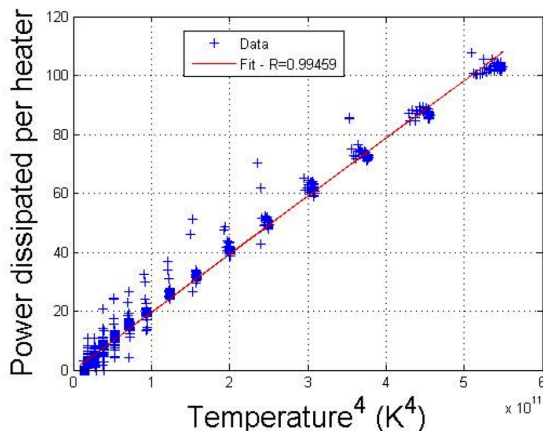


Figure 3.9: Black body radiation is the dominant thermal loss mechanism at high temperatures. When the apparatus is run at 1000 °C the radiant heat is sufficient to warm the metal bell jar to 50 °C.

3.3 Challenges of Phase Transition Seebeck

Though materials based on Ag_2Se and Cu_2Se are of great current interest in thermoelectrics, they are not new materials. Both are binary chalcogenides and are even present as uncommon earth minerals as Berzelianite (Cu_2Se) and Naumanite (Ag_2Se). Despite this rich history, my work is the first to successfully measure their phase transition thermoelectric properties correctly. I provide an example of literature attempts to measure their Seebeck coefficient in Figure 3.10. The plot is from Okamoto (1971) [144] and includes data from Bush and Junod (1959) [27]. These two data sets used different approaches and these different approaches led to different errors. My understanding of these two approaches and their errors indicated that a different technique was necessary. This method is described in detail in section 3.4 below.

Okamoto's data superficially resembles my own, but his approach suffered from systemic problems. First, he used a two point Seebeck geometry with the heater blocks made of copper. This raises the possibility of transfer of copper in and out of Cu_2Se from the heater blocks; thereby making the exact stoichiometry uncertain. He also used a variation of the single point Seebeck method that I will call the *single ramp technique*. Each data point he measured was derived from a single ΔV ,

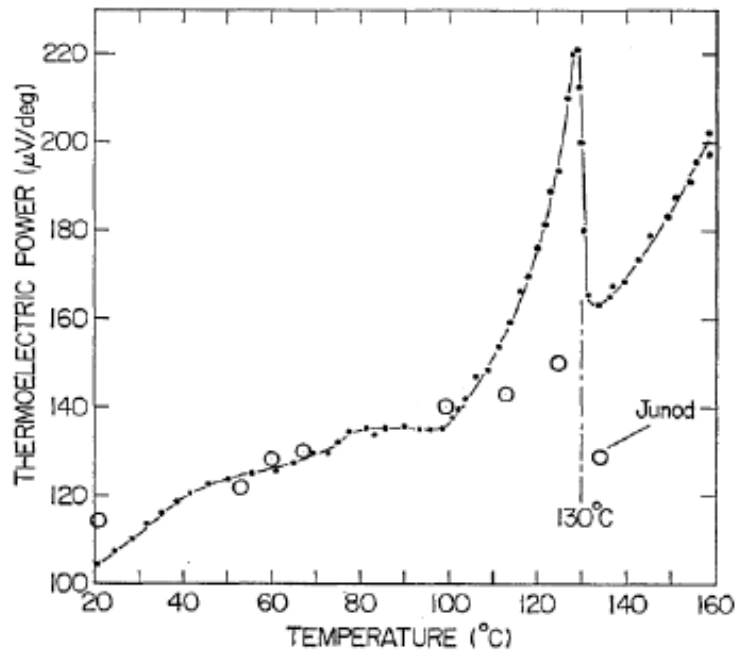


Figure 3.10: Literature Seebeck (Thermoelectric Power) data on Cu_2Se . Image extracted from Okamoto (1971) [144]. Data points labeled Junod originally from Bush & Junod [27]. Okamoto's data was obtained using a single point technique. Bush & Junod's data was obtained using an oscillation technique. Both were insufficient for correct determination of the Seebeck Coefficient.

ΔT pair. Therefore any offset temperature or voltage would skew the value as per Equation 3.1. The ΔT used was up to 5 K and that therefore limits the resolution at or near the phase transition. That limitation is sufficient for determining the *existence* of a phase-transition anomaly; it may be insufficient for the proper calculation of zT . Methodologically, he ramped the average temperature at a constant (but unreported) rate while performing single point Seebeck data. He observed the peak in Seebeck, but there is no way to determine whether the data is accurate or chimerical.

Bush and Junod used the oscillation method. Variants of this technique are in standard use at Caltech, JPL, and in commercially available instruments. Ideally in this technique, the sample is kept at an average temperature (\bar{T}), while the voltage (V) is measured at various temperature differences (ΔT). The Seebeck coefficient (α) is taken as the slope of the best fit line to V and ΔT data. This standard method is not ideal for the assessment of phase transition properties for three reasons: drift in temperature during a Seebeck oscillation, the instability due to kinetics associated with the phase transition, and limits on its temperature resolution. Bush and Junod caught hints of the phase transition anomaly using this technique, but without the resolution necessary to make a definitive statement.

The finite temperature shifts of an oscillation sequence causes errors when measuring near a phase transition. To make a Seebeck fit, the temperature of the two sides of the sample must deviate through a range of ΔT 's. This range is typically 5 K or 6 K to ensure a good Seebeck fit. For a typical sample with a slowly varying Seebeck coefficient this range is insufficient to cause a significant error. However, near the peaked Seebeck second order transition of Cu_2Se or the step change in Seebeck at a first order transition, the finite temperature range used can be problematic.

The essence of a Seebeck fit is to make the approximation to a set of N ($V, \Delta T$) points taken at the same \bar{T} .

$$\alpha \equiv \frac{\partial V}{\partial T} = \frac{1}{N} \sum_i \frac{\Delta V_i - V_{Dark}}{\Delta T_i}, \quad (3.2)$$

if N points are measured. The process is therefore to approximate to a Taylor expan-

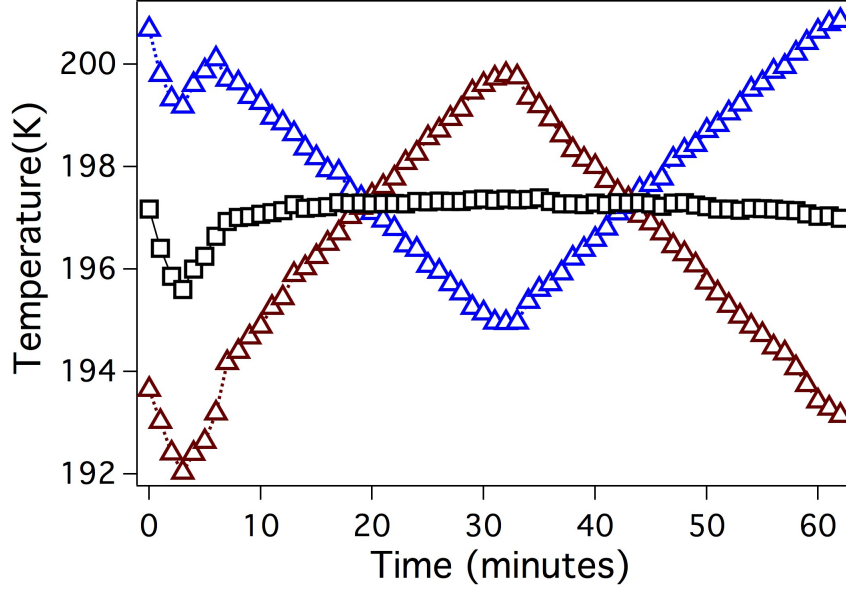


Figure 3.11: Sample oscillation sequence. Magenta and blue triangles are the temperature at the top and bottom side of the sample. Black squares are the average temperature. There is a small variation of average temperature that is correlated with the direction of ΔT .

sion to first order, and so intuitively as ΔT becomes larger this approximation error gets more and more significant. The full Taylor expansion for the Seebeck coefficient about \bar{T} is:

$$\alpha(T) = \alpha(\bar{T}) + (T - \bar{T}) \frac{\partial \alpha}{\partial T} + \frac{1}{2} (T - \bar{T})^2 \frac{\partial^2 \alpha}{\partial T^2} + \dots \quad (3.3)$$

Defining $\delta T = T - \bar{T}$, the corresponding voltage error at a given ΔT is:

$$V_{error}(\Delta T) = \alpha(T) - \alpha(\bar{T}) = \int_{-\Delta T/2}^{\Delta T/2} d\delta \left(\delta T \frac{\partial \alpha}{\partial T} + \frac{1}{2} \delta T^2 \frac{\partial^2 \alpha}{\partial T^2} \right) \quad (3.4)$$

Inspection of Equation 3.4 reveals that the odd terms of Equation. 3.3 do not contribute to V_{error} . However, if there is a correlation between the deviations in δT and ΔT , there will be an error term on order of $\frac{\partial \alpha}{\partial T} \langle \delta T^2 \rangle^{1/2}$. Inspection of oscillation data from our apparatus reveals that $\langle \delta T^2 \rangle^{1/2}$ is of order 0.25 K. This problem is therefore significant near 406 K in Cu_2Se — the temperature of the zT peak — at which $\alpha = 140 \mu\text{V}/\text{K}$ and $\frac{\partial \alpha}{\partial T} = 20 \mu\text{V}/\text{K}^2$. It may result in a several percentage error.

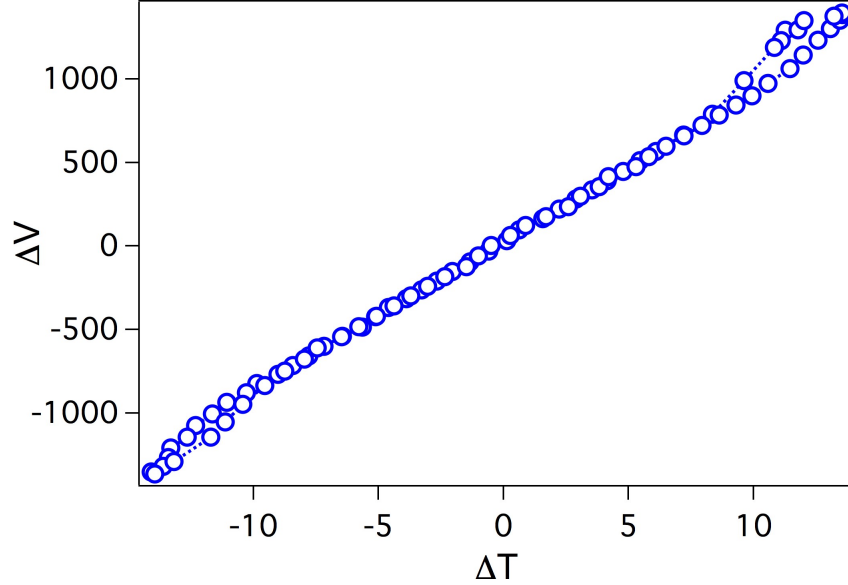


Figure 3.12: Raw Seebeck data for Cu_2Se measured at $\bar{T} = 410\text{K}$. There is a distinct cubic contribution and deviations from a consistent curve.

Ignoring correlations between ΔT and \bar{T} , we can simplify Equation 3.4 as:

$$V_{error} = \frac{\Delta T^3}{24} \frac{\partial^2 \alpha}{\partial T^2} \quad (3.5)$$

As Seebeck is typically cited with a 10% error, the condition for this effect being significant is:

$$\frac{\partial^2 \alpha}{\partial T^2} = 0.72 \alpha \Delta T^{-2} \quad (3.6)$$

While for a typical thermoelectric material this error is small, for phase transition materials it can be significant. For a typical thermoelectric material α varies gradually while temperature $\frac{\partial^2 \alpha}{\partial T^2}$ is very small ($< .01 \mu\text{V}/\text{K}^3$). Even in the most extreme case with $\alpha = 100 \mu\text{V}/\text{K}$ and $\frac{\partial^2 \alpha}{\partial T^2} = 0.1 \mu\text{V}/\text{K}^3$, the condition of Equation 3.6 is met only for $\Delta T > 25\text{K}$. However, near the Seebeck peak of Cu_2Se $\frac{\partial^2 \alpha}{\partial T^2} \approx 3 \mu\text{V}/\text{K}^2$ and the relevant ΔT from Equation 3.6 is the only 5 K. This error can be seen in Figure 3.12.

In the case of a step change in Seebeck at a first order transition, the Taylor expansion formalism of Equation 3.3 must be modified to contain two piecewise functions

above and below the phase transition. These piecewise functions will be slowly varying, thereby making further Taylor expansion unnecessary for the argument above. Raw Seebeck plots in which a portion of the ΔT are above and below the phase transition are difficult to analyze. For a typical oscillation through a phase transition the resulting data will be disjointed and non-linear.

During a typical Seebeck oscillation \bar{T} deviates slightly from its average value, as can be seen in Figure 3.11. These deviations occur in the system described above due to imperfect PID control and the use of separate thermocouples for temperature control and temperature measurement. The Seebeck error for a single point will be only of order $\frac{\partial\alpha}{\partial T}\Delta T$; in typical thermoelectric materials (*e.g.*, $\frac{\partial\alpha}{\partial T} = 1 \mu\text{V}/\text{K}^2$, $\alpha = 100 \mu\text{V}/\text{K}$, this error is only a few percent. The point by point error itself will only effect the overall Seebeck if there is a correlation between ΔT and \bar{T} . Otherwise these terms in Equation 3.2 will average to zero, and the leading term will be that of $\frac{\partial^2\alpha}{\partial T^2}$. As argued above, this term is small for typical thermoelectrics.

For phase transition thermoelectrics the drift in \bar{T} during an oscillation measurement can have large effects. Near the Seebeck peak of Cu_2Se $\frac{\partial\alpha}{\partial T}\Delta T$ is as much as 8% of α . The result of this error would be inaccuracies (reduction) in the peak value of Seebeck measured. For a first order transition such as Ag_2Se , crossing the phase transition temperature will result in errors greater than 10% in measured voltage.

3.4 The Multi-Ramp Seebeck Technique

To minimize error and increase the resolution of the Seebeck data near the phase transition, a modification to the standard Seebeck metrology was made. I named this technique the "Ramp Seebeck" technique. While in the Oscillation Seebeck technique \bar{T} is held nominally constant while ΔT is varied and the resultant voltage measured, in the Ramp Seebeck technique ΔT is held nominally fixed while the \bar{T} is steadily increased or decreased.

During each ramp the $(\Delta T, V)$ pairs are measured continuously. In our apparatus the effective \bar{T} steps between data points was on average 0.25 K when ramping at 15

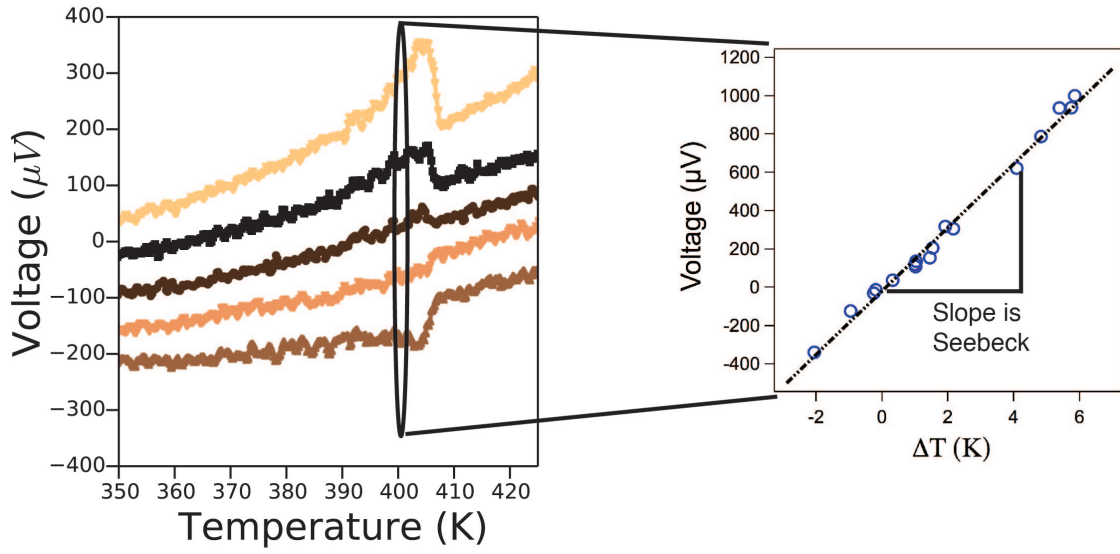


Figure 3.13: Data from multiple ramp sequences are combined point by point to create ΔV versus ΔT from which point by point Seebeck values may be extracted

K/min. Each separate ramp has a slightly different set of \bar{T} values. The $(\bar{T}, \Delta T, V)$ data sets from each ramp were interpolated onto the same \bar{T} values for comparison. The spacing of the new \bar{T} was the average temperature step between data points, as that sets a resolution limit on the measurement procedure.

This process is illustrated in Figure 3.13, in which the coefficient is plotted point by point without compensation for the voltage offset. If data from a single \bar{T} is explicitly plotted, then a raw Seebeck plot (V vs ΔT) is created from which a single (\bar{T}, α) point may be determined. This process is done at all temperatures using the combined heating and cooling data and is illustrated in Figure 3.13.

The proof of the superiority of the multi-ramp method for this problem is its superior results. In Figure 3.14 I plot the Seebeck coefficient and dark temperature measured on Cu_2Se by both the oscillation and ramp method. While the oscillation method shows the general trend of the anomalous Seebeck peak, it lacks sufficient resolution and clarity to fully describe the phase transition region. The temperature intercept is also of much smaller magnitude during the ramp measurement. The reason for this happy situation is unclear, but it is possible that the multiple ramps through the phase transition temperature allow the thermal contacts to stabilize into

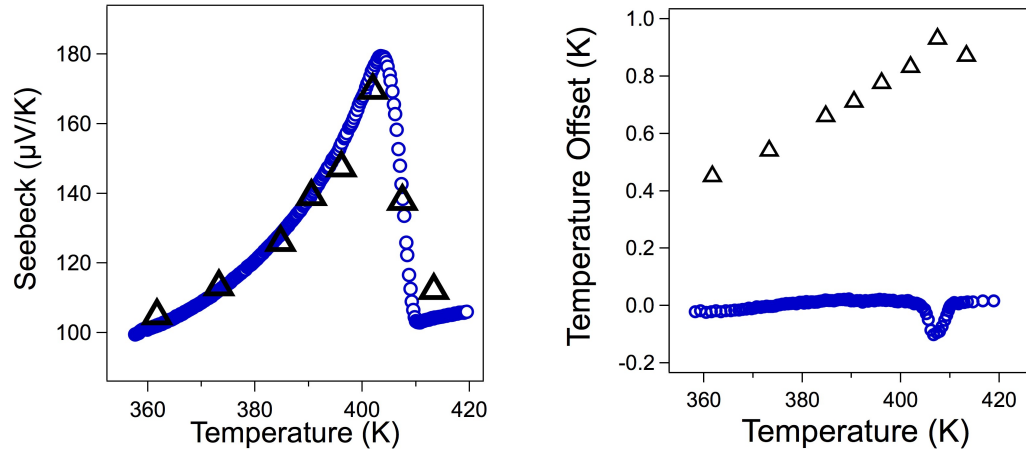


Figure 3.14: Comparison of oscillation (black triangles) and multi-ramp method data (blue circles) for Cu_2Se in proximity to its phase transition. The ramp data is superior.

a better position. Therefore the thermal contacts are superior and thus the Seebeck value more trustworthy for data using the multi-ramp technique rather than the oscillation technique.